Green
Chemistry

Accepted Manuscript

This article can be cited before page numbers have been issued, to do this please use: W. Deng, P. Wang, B. wang, Y. Wang, L. Yan, Y. Li, Q. Zhang, Z. Cao and Y. Wang, *Green Chem.*, 2018, DOI: 10.1039/C7GC02975F.

Volume 18 | Number 7 | 7 April 2016 | Pages 1821–2242

Green
Chemistry

Cutting-edge research for a greener sustainable future
www.rsc.org/greenchem

ISSN 1463-9262

ROYAL SOCIETY OF CHEMISTRY

CRITICAL REVIEW
G. Chatel et al.
Heterogeneous catalytic oxidation for lignin valorization into valuable chemicals: what results? What limitations? What trends?

175 YEARS

ROYAL SOCIETY OF CHEMISTRY

View Article Online
DOI: 10.1039/C7GC02975F

Green Chemistry

ARTICLE

Transformation of cellulose and related carbohydrates into lactic acid with bifunctional Al(III)-Sn(II) catalysts

Received 00th January 20xx,
Accepted 00th January 20xx

DOI: 10.1039/x0xx00000x

www.rsc.org/

Weiping Deng, Pan Wang, Binju Wang, Yanliang Wang, Longfei Yan, Yanyun Li, Qinghong Zhang,* Zexing Cao and Ye Wang*

Catalytic transformation of cellulose into valuable chemicals such as lactic acid under mild conditions represents a promising route for efficient utilization of renewable biomass. Here, we report that the combination of Al(III) and Sn(II) cations can efficiently catalyse the conversion of cellulose and related carbohydrates into lactic acid in water. The Al(III)–Sn(II) is the most efficient combination for lactic acid formation among many dual cations investigated. Al(III) and Sn(II) with a molar ratio of 1/1 work cooperatively, providing lactic acid with yields of 90%, 81% and 65% in the conversions of fructose, glucose and cellulose, respectively. The formation of lactic acid involves a series of tandem steps including the hydrolysis of cellulose to glucose, the isomerisation of glucose to fructose, the retro-aldol fragmentation of fructose to C_3 intermediates and the subsequent conversion of the C_3 intermediates to lactic acid. Our experimental and computational studies suggest that Al(III) mainly catalyses the isomerisation of glucose or the C_3 intermediates, whereas Sn(II) is primarily responsible for the retro-aldol fragmentation. The combination of the two cations enables the reaction to proceed smoothly with few side reactions, providing outstanding catalytic performances for lactic acid production from cellulose or the related carbohydrates.

1. Introduction

The catalytic transformation of renewable biomass resources, in particular the most abundant and non-edible lignocellulosic biomass, into chemicals, fuels and materials is the key to establishing a sustainable chemical society.[1-4] Cellulose is the major component of lignocellulosic biomass, and thus the efficient transformation of cellulose under mild conditions plays an essential role in biomass valorisation.[5] However, the direct transformation of cellulose under mild conditions is difficult due to the robust crystalline structure of cellulose. Furthermore, various C-C and C-O bonds with similar bond energies exist in cellulose molecules, making the selective cleavage of specific chemical bonds to obtain a particular valuable chemical highly challenging.

In the past decades, tremendous endeavours have been devoted to developing efficient catalytic systems for the conversion of cellulose or the related carbohydrates into useful platform compounds such as 5-hydroxymetyl furfural (HMF),[6,7] polyols,[8-12] and organic acids.[13-18] Among these transformations, the synthesis of value-added organic acids has received growing interests,[13-18] because the majority of elements such as carbon and oxygen can be maintained in the acids, which is in good agreement with the principle of high atomic economy. Moreover, the formation of organic acids usually occurs under non-reductive conditions and does not consume expensive hydrogen.

Lactic acid, which is one of the most versatile bio-based chemicals, has found a wide range of applications in food, pharmaceutical, cosmetic and chemical industries.[15,19] As a key building block, lactic acid can be facilely transformed into other important chemicals in chemical industry such as acrylic acid, pyruvic acid, propylene glycol, 2,3-pentanedione and acetaldehyde.[15,19] Furthermore, lactic acid is the monomer of poly(lactic acid), a bio-degradable plastic and a potential candidate to replace petroleum-derived polymers.

Currently, lactic acid is primarily produced through the conventional biotechnological process *via* fermentation of carbohydrates (usually glucose and sucrose).[15] Such a fermentation process suffers from high enzyme cost, low space-time yield, undesirable waste effluents and large complexity in purification. Moreover, the fermentation is restricted to the transformation of hexose sugars or easily hydrolysable poly- and disaccharides from starch. In contrast, the chemical catalysis possesses advantages of easiness in catalyst design and reaction condition engineering to optimize the performance. Moreover, the synthesis of lactic acid directly from cellulose is also possible via chemical catalysis.

The development of efficient chemocatalytic systems for lactic acid synthesis from cellulose or its derived carbohydrates has attracted much attention in recent years. Many studies reported that the use of alkalis (e.g., NaOH, KOH) as catalysts under supercritical or subcritical conditions could break down the C-C bonds in glucose, forming alkali lactates.[20-23] However, the alkali system usually shows low selectivity to lactate, and

---

State Key Laboratory of Physical Chemistry of Solid Surfaces, Collaborative Innovation Center of Chemistry for Energy Materials, National Engineering Laboratory for Green Productions of Alcohols, Ethers and Esters, College of Chemistry and Chemical Engineering, Xiamen University, Xiamen 361005, China. E-mail: zhangqh@xmu.edu.cn; wangye@xmu.edu.cn; Fax: +86-592-2183047; Tel: +86-592-2186156

† Electronic Supplementary Information (ESI) available: See DOI: 10.1039/x0xx00000x

the salts of many other acids such as formic, acetic, oxalic and levulinic acids are also generated because of the severe reaction conditions (> 473 K). Co-catalysts have been employed to improve the performance of alkali catalysts. Huang and co-workers reported that a polymer of imidazole and epichlorohydrin in combination with NaOH aqueous solution could offer a lactate yield of 63% during the conversion of glucose at 373 K.[24] The polymer was proposed to function as weak Lewis acid sites to coordinate with key intermediates, thus facilitating the formation of lactate. Choudhary et al. claimed that a magnesia-supported copper accelerated the conversion of glucose to lactate in aqueous alkaline solution, affording a lactate yield of 70% at 393 K.[25] Barium hydroxide could also work as a catalyst for the conversion of glucose, affording a lactate yield up to 95% after 48 h reaction, but a high ratio of $Ba(OH)_2$ to glucose (10/1) was required.[26]

Lewis acid-based catalysts have also been reported for the production of lactate from glucose or the related carbohydrates.[27-29] By incorporating Sn(IV) ions into the framework of zeolite beta, Taarning and co-workers succeeded in the conversion of glucose and sucrose into methyl lactate in methanol.[30] A methyl lactate yield of 64% was attained in the conversion of sucrose at 433 K for 20 h. The lactate selectivity for Sn-beta could be further enhanced to 75% with the assistance of K_2CO_3,[31] which was supposed to neutralize the Brønsted acid sites in zeolites, thus inhibiting the Brønsted acid-catalysed side reactions. Sn(IV)-grafted mesoporous silica modified with carbon also catalysed the transformation of glucose, fructose and sucrose in methanol to methyl lactate.[32] Recently, a gallium-doped zeolite Y catalyst was reported to offer a methyl lactate yield of 58% from cellulose in supercritical methanol (553 K).[33] The harsh reaction conditions may facilitate side reactions (e.g., dehydration) by both methanol and substrate. Efficient catalytic systems that are capable of transforming cellulose to lactic acid directly in non-alkaline aqueous solution are still scarce. Zirconia,[34] tungstated zirconia-alumina,[35] and niobium-modified aluminium hydroxide fluorides[36] were disclosed to catalyse the direct conversion of cellulose under hydrothermal conditions, but the selectivity of lactic acid was low. Lanthanide triflates[37] and erbium-exchanged montmorillonite[38] showed high yields of lactic acid, but these systems either employed high-cost catalysts or suffered from low catalyst stability.

In addition to heterogeneous catalysis, homogeneous catalysis has also attracted much attention as an important tool for the transformation of biomass.[39] In particular, the soluble catalyst can interact better with the linkage targeted for depolymerisation in cellulose. The molecular catalysis with well-defined active sites can provide deeper mechanistic insights. In a previous paper,[40] we reported that a simple metal cation, Pb(II), could efficiently catalyse the direct transformation of cellulose in aqueous medium, producing lactic acid with a yield as high as 65% at 463 K. However, the toxicity of Pb(II) is unfavourable for its future application. Thus, it is highly attractive to develop more environmental friendly catalytic systems for the transformation of cellulose into lactic acid. Furthermore, some aspects of reaction mechanism are still unclear, limiting the rational design of highly selective catalysts. The formation of lactic acid involves the cleavage of one C-C bond. The cleavage of C-C bond may occur at different positions in the skeleton of glucose, the monomer of cellulose. How to control the selectivity of C-C cleavage is of fundamental significance. Here, we report our recent finding that a combination of Al(III) and Sn(II) is highly efficient for catalytic transformations of cellulose and the related carbohydrates into lactic acid in water. Both experimental and computational studies are carried out to understand in-depth the reaction mechanism and catalytic functions of Al(III) and Sn(II). We attempt to gain insights into the precise cleavage of the C-C bond in carbohydrates to form target product with few side reactions through the present simple homogeneous catalytic system.

2. Experimental

2.1. Materials and general methods. Most of the inorganic chemicals used in this work, such as $AlCl_3$, $Al_2(SO_4)_3$, $SnCl_2$, SnI_2, $SnBr_2$, $SnSO_4$, $Zn(NO_3)_2$, $FeCl_2$, $Mn(NO_3)_2$, $Cu(NO_3)_2$, $NiCl_2$ and $Co(NO_3)_2$, were purchased from Sinopharam Co. $In(NO_3)_3$, $Ga(NO_3)_3$ and organic compounds such as cellulose, D-glucose, D-fructose, glyceraldehyde, dihydroxyacetone, pyruvaldehyde were purchased from Alfa Aesar. The obtained crystalline cellulose was typically ball-milled on a SFM-1 Desk-top planetary ball miller (MTI Corporation) for 48 h before use.

Fourier-transform ion cyclotron resonance (FT-ICR) mass spectrometry measurements were performed on a Bruker APEX IV 7.0T FT-ICR mass spectrometer in positive ion mode equipped with an external electrospray ionisation (ESI) source. $AlCl_3$ or $SnCl_2$ was dissolved in water to obtain a concentration of approximately 0.15 mmol L^{-1}. This solution was electrosprayed from a capillary biased at 4400 V. The scan range of m/z was from 100 to 600. An accuracy of m/z of 1×10^{-5} was achieved. Matrix-assisted laser desorption ionisation time of flight (MALDI-TOF) analysis was conducted over a range of 1-2000 on Bruker MALDI-TOF mass spectrometer. 2,5-Dihydroxybenzoic acid was used as the matrix.

2.2. Catalytic reaction. Conversions of cellulose, possible hexose and triose intermediates and other biomasses were performed in a batch-type Teflon-lined stainless-steel autoclave. As an example for the conversion of cellulose, the catalyst and the powdery cellulose were added to the reactor, which had been pre-charged with deionised water. After the introduction of N_2 with a pressure of 3 MPa, the reactor was placed in an oil bath. When the system reached the reaction temperature (typically 463 K), the reaction was initiated by vigorous stirring. After a fixed time, the reaction was quickly terminated by cooling the reactor to room temperature in cold water. The liquid products were analysed by a high-performance liquid chromatography (HPLC, Shimazu LC-20A) equipped with an RI detector and a Shodex SUGARSH-1011 column (8×300 mm) using a dilute H_2SO_4 aqueous solution as the mobile phase. The conversion was calculated on the basis of the molar difference between the substrate before and after each reaction. The yields of main products, such as lactic acid, glucose, fructose, HMF and levulinic acid, were calculated from the percentage of carbon moles of products in the total carbon moles of the substrate.

2.3. Theoretical computation. All of the computations were performed with the Gaussian 09 software package. The geometries of the transition states, reactants and

View Article Online
DOI: 10.1039/C7GC02975F

intermediates involved in the reaction were optimized using a hydrated cluster in conjunction with the continuum solvation model of SMD at the B3LYP/6-31G(d) level of theory (the LanL2DZ-ECP basis set was employed for Al and Sn). Harmonic frequency calculations were performed at the equilibrium geometries to confirm first-order saddle points and local minima on the potential energy surfaces and to estimate the zero-point energy (ZPE) as well as the thermal and entropic corrections at 298.15 K and 1 atm. The correlation between the stable structures and the transition states was verified by analysing the corresponding imaginary frequency mode as well as by limited intrinsic reaction coordinate (IRC) calculations. The relative energies of the B3LYP/6-31G(d)-optimized structures were further refined by single-point calculations at the B3LYP/6-311++G(d,p) level (the polarized LANL2DZdp ECP basis set was employed for Al and Sn) with inclusion of solvent effects. Natural bond orbital (NBO) analyses at the B3LYP/6-311++G(d,p) level were performed to determine the atomic charge populations. For estimation of the Gibbs free energy, direct calculations in combination with frequency analysis in solution were performed, which had been verified to be a correct and practical approach[41] especially when liquid-phase and gas-phase structures differed significantly or when the stationary points present in the liquid solution could not survive in the gas phase. The B3LYP method was compared with several other popular density functional theoretical (DFT) methods including B3PW91, B97-D, M06, X3LYP and M06-2X for the isomerisation of glucose to its enol form, and B3LYP was found to be adequate for the present mechanistic study. In addition to 298.0 K, thermal corrections were also assessed at 463.0 K to explore the temperature effect on the Gibbs free energy, and the temperature effect was not remarkable here.

3. Results and discussion

3.1. Catalytic behaviours of single- and dual-metal cations for conversions of cellulose and related carbohydrates to lactic acid

We first examined catalytic performances of various easily accessible, cheap and less toxic single metal cations including Al(III), In(III), Mn(II), Fe(II), Co(II), Ni(II), Cu(II), Zn(II) and Sn(II) for the conversion of fructose, a key cellulose-derived hexose, in water medium. No lactic acid was formed without a cation. Among all the single metal cations investigated, Al(III) was the most efficient, providing a lactic acid yield of 41% at 463 K for 2 h (Fig. 1). Sn(II), In(III), Zn(II) and Mn(II) also catalysed the transformation of fructose to lactic acid with moderate yields of 25-35%. Other metal ions such as Co(II), Fe(II), Ni(II) and Cu(II) were less efficient for lactic acid formation. Then, we investigated different combinations of dual metal cations with a molar ratio of 1/1 for the conversion of fructose at 463 K, and the results for the combinations containing Al(III) are displayed in Fig. 1. An outstanding lactic acid yield of 90% was achieved using Al(III)-Sn(II). The Al(III)-Sn(II) combination is also the most efficient for the conversion of fructose to lactic acid among many other dual-cation combinations (Fig. S1, ESI†).

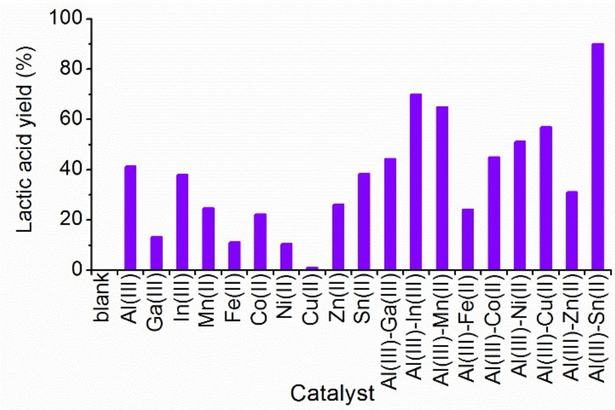

Fig. 1 Catalytic conversion of fructose into lactic acid catalysed by various single cations or dual-cation combinations. Reaction conditions: fructose, 0.56 mmol; single or dual cations, 0.10 mmol; H_2O, 20 mL; N_2, 3 MPa; 463 K; 2 h. For dual cations, the molar ratio of the two components was 1/1.

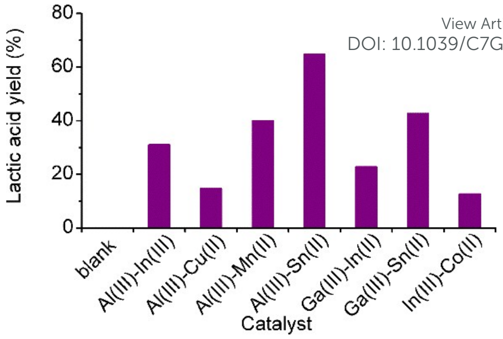

Fig. 2 Catalytic conversion of cellulose catalysed by dual cations. Reaction conditions: cellulose, 0.10 g (glucose unit, 0.62 mmol); dual-metal cations (ratio = 1/1), 0.10 mmol; H_2O, 20 mL; N_2, 3 MPa; 463 K; 2 h.

Subsequently, we performed conversion of ball-milled cellulose in water using the dual-cation catalysts that were efficient for the conversion of fructose. The Al(III)-Sn(II) also exhibited the best performance for the formation of lactic acid from cellulose, followed by Ga(III)-Sn(II), Al(III)-Mn(II) and Al(III)-In(III) combinations (Fig. 2). A lactic acid yield of 65% was attained in the conversion of cellulose at 463 K for 2 h with the Al(III)-Sn(II) catalyst. We have checked whether the counter anions influence catalytic performances. Almost the same yield of lactic acid was obtained during the conversion of cellulose at 463 K using the combination of different salts of Al(III) and Sn(II) (Table S1, ESI†). Thus, Al(III) and Sn(II) cations are the true catalytically active species for the formation of lactic acid.

The Al(III)-Sn(II) catalyst was further applied to the conversion of microcrystalline cellulose and other biomasses or carbohydrates such as starch, inulin, cellobiose and glucose. As expected, the microcrystalline cellulose was more difficult to be converted than the ball-milled cellulose, and we obtained a lactic acid yield of 36% from the microcrystalline cellulose after 2 h of reaction at 463 K (Table S2, ESI†). For other biomasses or carbohydrates, lactic acid yields of 71% to 89% were obtained (Table S2, ESI†), which were comparable or even higher than those obtained using the Pb(II) catalyst reported in our previous paper under the same conditions.[40] In other words, the present dual-cation catalyst can work as a more environmental benign and efficient homogeneous catalyst for the conversion of various biomasses to lactic acid.

We further performed the conversions of glucose and fructose with high concentrations (2.5-10 wt%) using the Al(III)-Sn(II) catalyst. A lactic acid yield of ~50% could be achieved for the conversion of either glucose or fructose with a concentration of 2.5 wt% (Table S3, ESI†). The further

View Article Online
DOI: 10.1039/C7GC02975F

increase in the concentration of sugars decreased the lactic acid yield. Possibly, the relatively higher concentration of lactic acid formed in the concentrated sugar solution may significantly influence the pH value of the solution, thus affecting the catalytic behaviours.

We have investigated the effect of pH on catalytic behaviours of the Al(III)-Sn(II) catalyst. Since both Al(III) and Sn(II) chlorides used in the present work were slightly hydrolysed in water, the initial pH value of the reaction solution was around 2.8. The formed Brønsted acids would favour the hydrolysis of cellulose. We further regulated the pH value in a range of 0.86-7.6 by using either HCl or NaOH and examined the effect of pH value on the conversion of glucose at 453 K. At a pH value of ≤ 2.8, glucose could be completely converted (Table 1). However, a lower pH caused a decrease in the selectivity of lactic acid and an increase in that of levulinic acid. The formation of humins was also observed. This suggests that an excess amount of Brønsted acids may accelerate undesirable side reactions and are unbeneficial to the formation of lactic acid. We further found that a higher pH value (> 2.8) was also unfavourable. Both the glucose conversion and the lactic acid selectivity decreased by increasing the pH from 2.8 to 7.6. It is likely that the higher pH value reduced the concentrations of Al(III) and Sn(II) cations by increasing those of the corresponding hydroxide species via hydrolysis. Therefore, a proper pH value is required not only to avoid the side reactions such as the formation of levulinic acid and humins at a lower pH value but also to keep a balance between metal cations and their hydroxide species to ensure the high efficiency for the formation of lactic acid.

3.2. Reaction pathways for the formation of lactic acid

The effect of the concentration of Al(III)-Sn(II) (Al/Sn molar ratio = 1/1) on catalytic performance for the conversion of cellulose at 463 K is displayed in Fig. 3. Cellulose could also be converted in the absence of metal cations under hydrothermal conditions, mainly producing glucose and HMF. No lactic acid was formed. It is known that H_3O^+ ions can be reversibly generated in hot water because of the increased ionisation constant under hydrothermal conditions.[9,42] The hydrolysis of cellulose to glucose is probably catalysed by such in-situ generated protons.[9] HMF may be formed by acid-catalysed dehydration of fructose, which probably arises from the isomerisation of glucose. The introduction of Al(III)-Sn(II) cations into the reaction system not only increased the conversion of cellulose but also significantly changed the product selectivity. The formation of lactic acid was triggered by the presence of dual cations and the lactic acid selectivity increased upon increasing the concentration up to ~5 mmol L^{-1} at the expense of the selectivities of glucose and HMF. The catalyst concentration of ≥ 2.8 mmol L^{-1}, accounting for ≥ 9.0 mol% of glucose units in cellulose, was needed to achieve ≥ 50% selectivity of lactic acid. These results suggest that several reactions including hydrolysis, isomerisation and dehydration may occur under hydrothermal conditions, whereas the dual cations not only enhance the conversion of cellulose but also catalyse the formation of lactic acid via cleavage of the C-C bond.

Table 1 Effect of pH value of the reaction solution on catalytic behaviours of Al(III)-Sn(II) dual cations for the conversion of glucose[a]

pH	Conv. (%)	Yield (%)			
		Fructose	Lactic acid	Levulinic acid	Others[b]
0.86	100	0	5.6	26	7.2
1.8	100	0	31	15	5.0
2.8	100	0	81	4.4	3.0
4.0	99	0.7	52	2.9	3.6
7.6	90	9.5	10	1.3	16

[a] Reaction conditions: glucose, 0.10 g (0.56 mmol); Al(III)-Sn(II) cations [Al(III)/Sn(II) molar ratio = 1/1], 0.10 mmol; H_2O, 20 mL; N_2, 3 MPa; 453 K; 2 h. $AlCl_3$ and $SnCl_2$ were used. [b] Others include HMF, glyceric acid, acetic acid and formic acid. The formation of humins caused the low carbon balance at low pH values (< 2.8), while at a high pH value (> 2.8), some unknown products led to the poor carbon balance.

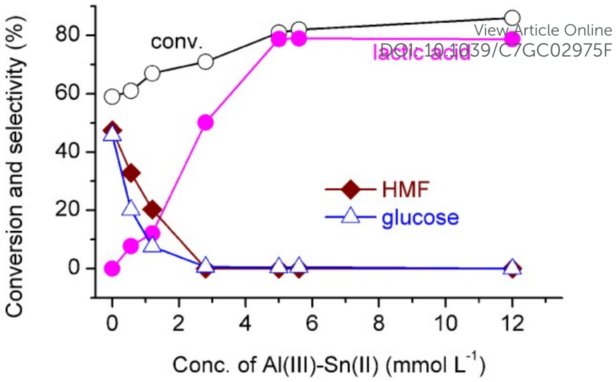

Fig. 3 Effect of concentration of Al(III)-Sn(II) cations on catalytic behaviours for the conversion of cellulose. Reaction conditions: cellulose, 0.10 g (glucose unit, 0.62 mmol); H_2O, 20 mL; N_2, 3 MPa; 463 K; 2 h. $AlCl_3$ and $SnCl_2$ were used. The molar ratio of Al(III)/Sn(II) was 1/1.

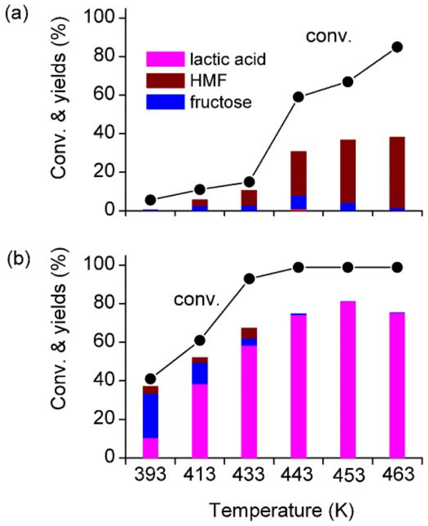

Fig. 4 Catalytic conversion of glucose at different temperatures. (a) In the absence of metal cation catalyst. (b) In presence of Al(III)-Sn(II) catalyst. Reaction conditions: glucose, 0.10 g (0.56 mmol); Al(III)-Sn(II) cations [Al(III)/Sn(II) molar ratio = 1/1], 0.10 mmol (in the presence of catalyst); H_2O, 20 mL; N_2, 3 MPa; 2 h. $AlCl_3$ and $SnCl_2$ were used.

View Article Online
DOI: 10.1039/C7GC02975F

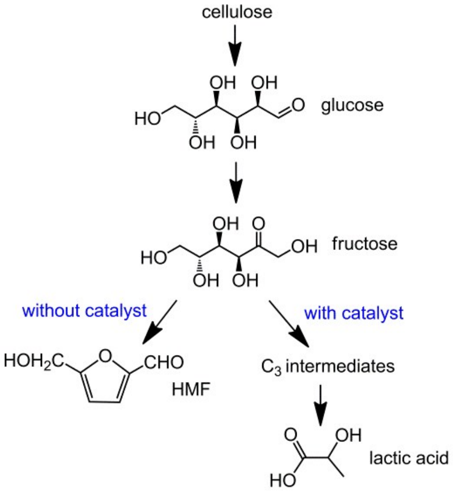

Fig. 5 Reaction pathways for the conversion of cellulose in the presence and absence of Al(III)-Sn(II) catalyst.

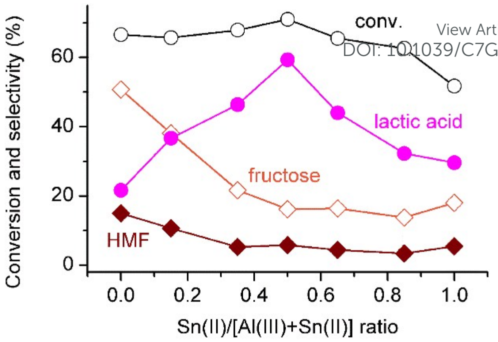

Fig. 6 Effect of Al(III)/Sn(II) molar ratio on catalytic performances for the conversion of glucose. Reaction conditions: glucose, 0.10 g (0.56 mmol); H_2O, 30 mL; N_2, 3 MPa; 423 K; 0.5 h. $AlCl_3$ and $SnCl_2$ were used. The total amount of Al(III) and Sn(II) was fixed at 0.10 mmol.

We carried out the conversion of glucose, a key intermediate during the transformation of cellulose, at different temperatures to gain more information about the reaction pathway. In the blank reaction, fructose and HMF were the major products, and HMF became the dominant product at higher temperatures (Fig. 4a). The reaction solution turned dark brown at higher temperatures, indicating the formation of undesired humins. The presence of Al(III)-Sn(II) significantly enhanced the conversion of glucose particularly at lower temperatures. The formation of fructose was remarkably accelerated at lower temperatures (393 and 413 K). The increase in temperature in the presence of Al(III)-Sn(II) catalyst resulted in the formation of lactic acid instead of HMF in the blank reaction. The yield of lactic acid from glucose was 81% at 453 K.

A detailed time-course analysis for the conversion of glucose at 423 K with Al(III)-Sn(II) catalyst revealed that fructose was initially formed as the primary intermediate (Fig. S2, ESI†). Upon prolonging the reaction time, the selectivity of fructose decreased and that of lactic acid increased simultaneously. Glyceraldehyde was formed with a low selectivity. It can be expected that retro-aldol fragmentation of fructose may break the C3-C4 bond at the middle of the molecule, yielding two C_3 intermediates, which may be readily converted to lactic acid or lactates.[38,40,43,44] Therefore, we propose reaction pathways in Fig. 5. In brief, the conversion of cellulose to lactic acid catalysed by the Al(III)-Sn(II) involves the following steps: the hydrolysis of cellulose to glucose, the isomerization of glucose to fructose, the retro-aldol fragmentation of fructose to C_3 intermediates and the subsequent isomerisation of C_3 intermediates into lactic acid. In the absence of a catalyst, the formation of HMF was mainly observed. HMF may be formed from fructose by dehydration.

3.3. Catalytic functions of Al(III) and Sn(II)

To clarify the roles of Al(III) and Sn(II) in each step, we investigated the effect of molar ratio of Sn(II)/Al(III) on the conversion of glucose at 423 K. As shown in Fig. 6, single Al(III) cation mainly catalysed the transformation of glucose to fructose, although HMF and lactic acid were also formed to some extent. Thus, it is reasonable to speculate that Al(III) cations are mainly responsible for the isomerisation of glucose to fructose. Upon the addition of Sn(II) cation, the selectivity of fructose decreased and that of lactic acid increased significantly. The selectivity of HMF became further lower in the presence of Sn(II). When the Sn(II)/Al(III) ratio reached 1/1, i.e., Sn(II)/[Al(III)+Sn(II)] ratio = 0.5, the selectivity and yield of lactic acid were the highest. A further increase in the ratio of Sn(II)/Al(III) rather caused a drop in the selectivity of lactic acid. At the same time, the conversion of glucose also decreased. Single Sn(II) cation could catalyse the conversion of glucose to lactic acid, but the selectivity was only 30%. The selectivities of fructose and HMF were also low in the presence of Sn(II) alone, and the formation of humins was observed.

To understand the catalytic function of Sn(II) deeply, we have performed the conversion of fructose in the presence of

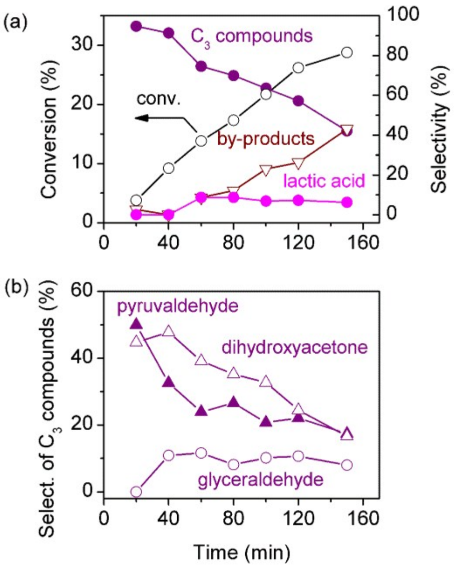

Fig. 7 Conversion of fructose in the presence of Sn(II) cation. (a) Conversion and product selectivity. (b) Selectivity of C_3 compounds. Reaction conditions: fructose, 0.10 g (0.56 mmol); Sn(II), 0.10 mmol; H_2O, 30 mL; N_2, 3 MPa; 383 K. $SnCl_2$ was used. The selectivity of by-products, which mainly included polymeric compounds and humins, were calculated by subtraction of the selectivity of known products with 100%.

single Sn(II) at 383 K. We adopted a relatively mild temperature to control the conversion of fructose with an attempt to gain information on the primary products from fructose catalysed by Sn(II). Fig. 7 shows that C_3 compounds are formed as the major products (selectivity, ~90%) at a short reaction time or at initial reaction stage. Thus, it becomes clear that Sn(II) catalyses the cleavage of C3-C4 bond in fructose to form C_3 compounds. The C_3 intermediates include pyruvaldehyde, dihydroxyacetone and glyceraldehyde (Fig. 7b). The prolonging of reaction time decreased the selectivity of these C_3 compounds, but the selectivity of lactic acid did not increase significantly at the same time in the presence of Sn(II) alone. Instead, polymeric by-products were formed. It has been reported that pyruvaldehyde can be facilely polymerized under mild conditions because of its reactive carbonyl groups.[45] Our MALDI-TOF analyses of the solid residue after the reaction suggest the polymerization of reactive C_3 aldehydes during our reactions (Fig. S3, ESI†).

We studied the conversions of three possible C_3 intermediates, glyceraldehyde (GLY), dihydroxyacetone (DHA) and pyruvaldehyde (PAD), to gain insights into the active species for the conversion of these C_3 intermediates. Table 2 displays that the three trioses can easily undergo intermolecular transformations into each other in water even without a metal cation catalyst. Glyceraldehyde is more active to be transformed in the absence of a catalyst, and this can explain our result that pyruvaldehyde and dihydroxyacetone have been observed as the major products during the conversion of fructose (Fig. 7b), although glyceraldehyde should be formed as a major product along with dihydroxyacetone by considering the C-C cleavage via retro-aldol fragmentation of fructose.

The presence of Al(III) significantly accelerated the conversion of each C_3 substrate, catalysing the formation of lactic acid with almost 100% yield (Table 2). Sn(II) also facilitated the conversion of each triose, but the selectivity of lactic acid was low. Humins were formed in the presence of Sn(II). We speculate that Sn(II) may catalyse the aldol condensation of aldehyde, e.g., pyruvaldehyde, with other aldehyde/alcohol intermediates,[45] leading to the formation of undesired polymeric by-products. Our time-course analyses for Sn(II)-catalysed conversions of pyruvaldehyde and glyceraldehyde showed the formations of glucose and fructose besides lactic acid and triose isomers (Tables S4 and S5, ESI†), confirming the occurrence of aldol condensation in the presence of Sn(II) alone. As compared to Sn(II) alone, the Al(III)-Sn(II) dual cations showed significantly higher selectivity of lactic acid during the conversion of glyceraldehyde, dihydroxyacetone or pyruvaldehyde, although the catalytic performance of Al(III) was better. Therefore, it is Al(III) but not Sn(II) that plays a dominating roles in the conversion of the C_3 intermediates into lactic acid.

Table 2 Catalytic performances of Al(III), Sn(II) and Al(III)-Sn(II) cations for the conversions of C_3 intermediates[a]

Catalyst	Substrate[b]	Conv. (%)	Yield (%)			
			GLY	DHA	PAD	Lactic acid
Blank	GLY	89	-	24	51	13
	DHA	57	0	-	40	14
	PAD	43	0	11	-	24
Al(III)	GLY	100	-	0	1.2	97
	DHA	100	1.7	-	0	98
	PAD	100	0	0	-	99
Sn(II)	GLY	93	-	0	37	45
	DHA	92	0	-	38	47
	PAD	71	0	13	-	48
Al(III)-Sn(II)	GLY	95	-	3.6	0	88
	DHA	89	0	-	5.5	83
	PAD	99	0	2.3	-	96

[a] Reaction conditions: substrate, 0.10 g; metal cation (or dual cations), 0.10 mmol; H_2O, 30 mL; N_2, 3 MPa; 413 K, 0.5 h. $AlCl_3$ and $SnCl_2$ were used. [b] GLY, DHA and PAD denote glyceraldehyde, dihydroxyacetone and pyruvaldehyde, respectively.

On the basis of the results described above, we propose that Al(III) mainly catalyses the isomerisation of glucose to fructose, while Sn(II) functions as the major active site for the retro-aldol fragmentation of fructose to form C_3 intermediates. The conversion of C_3 intermediates to lactic acid is mainly catalysed by Al(III), whereas Sn(II) led to the polymerisation of C_3 intermediates into humins. The two cations in the catalytic system work cooperatively for the conversion of glucose or other carbohydrates into lactic acid.

3.4. Mechanistic insights from DFT computations

We have carried out theoretical computations for the conversion of glucose to lactic acid in water to gain deeper insights into reaction mechanism and catalytic functions of Al(III) and Sn(II) in each elementary step. The present computational work employs a cluster-continuum model, which has been verified to be practicable for chemical reactions in aqueous solutions.[46,47] Our experimental studies have already indicated the following three main steps for the conversion of glucose into lactic acid: (1) the isomerisation of glucose to fructose, (2) the retro-aldol fragmentation of fructose to two C_3 intermediates and (3) the isomerisation of the C_3 intermediates into lactic acid. The detailed computational results are summarized in the electronic supplementary information (Figs. S4-S40, ESI†). Fig. 8 displays the mechanism based on the DFT calculation.

For the first step, i.e., the isomerisation of glucose, the reaction involves the shift of carbonyl group from C1 to C2 position. Generally, the intermolecular hydride shift and keto-

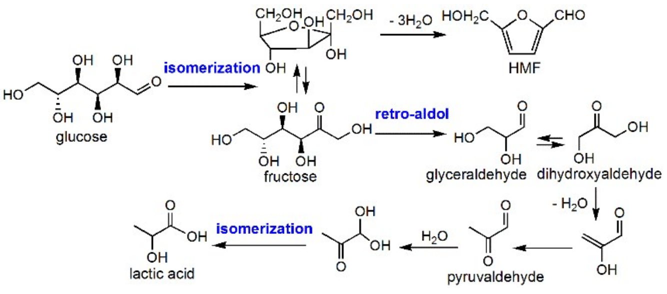

Fig. 8 Reaction mechanism based on the DFT computations for the conversion of glucose to lactic acid in water.

View Article Online
DOI: 10.1039/C7GC03075E

enol tautomerisation are two possible reaction mechanisms. In the alkali-catalysed isomerisation, the reaction has been proposed to proceed through a series of enolate intermediates produced after the deprotonation of the α-carbonyl carbon, indicating the keto-enol tautomerisation mechanism.[48,49] However, recent studies strongly suggest the intermolecular 1,2-hydride shift mechanism for the system with a transition metal cation catalyst.[50,51] By using ^{1}H and ^{13}C NMR isotope-labelled glucose, Davis and co-workers directly observed the hydrogen transfer from C2 to C1 in a Sn-based heterogeneous catalytic system.[52] Our previous studies revealed that the 1,2-hydride shift was more favourable for the isomerisation of glucose catalysed by homogeneous Pb(II) in aqueous solution.[40] Thus, we adopted the 1,2-hydride shift route for our computations. Moreover, our ESI-MS spectra revealed that the Al(III) cation tended to coordinate with two glucose molecules in the aqueous solution (Fig. S41, ESI†). Sn(II) could combine with either one or two glucose molecules, but the latter situation was the major case. Consequently, our computation models were established and optimized on the basis of these results (Fig. S4-S40, ESI†).

In the absence of a metal cation catalyst, the activation barrier, expressed by activation Gibbs energy ($\Delta G^{\neq}$), for the isomerization of glucose was calculated to be 24.1 kcal mol^{-1}.[40] The presence of Al(III) and Sn(II) lowered the activation Gibbs energy values to 20.9 and 19.9 kcal mol^{-1}, respectively (Table 3). This indicates that both cations are capable of enhancing this reaction. Besides the metal ions, we have also conducted the computations with hydroxyl-coordinated Al-OH and Sn-OH species, which have been reported as possible active species for the isomerization of glucose.[50,53-55] Table 3 shows that when Al(III)-OH and Sn(II)-OH are considered as active species instead of Al(III) and Sn(II), the activation Gibbs energy values decrease to 13.0 and 16.6 kcal mol^{-1}, respectively. The Al(III)-OH species shows the lowest activation barrier. This is in consistent with the experimental result that the aluminium species plays an important role in the isomerization of glucose.

The transformation of C_3 compounds resulting from the cleavage of C-C bond of fructose via retro-aldol fragmentation into lactic acid involves several tandem elementary steps including dehydration, hydration and isomerisation (Fig. 8). Among them, the isomerization via the 1,2-hydride shift mechanism has been demonstrated to be the rate-limiting step due to its large activation energybarrier.[40] Our computational results revealed that the energy barrier could be reduced in the presence of Al(III)-OH or Sn(II)-OH species (Table 3). Moreover, as compared to the Sn(II)-OH, the Al(III)-OH exhibited lower activation Gibbs energy, in consistent with the experimental result in Table 2.

Table 3 Activation Gibbs energy values for the key steps during conversion of glucose into lactic acid[a]

Reaction steps[b]	Non-catalytic route	Catalytic route by different species			
		Al(III)	Al(III)-OH	Sn(II)	Sn(II)-OH
Glucose to fructose	24.1	20.9	13.0	19.9	16.6
Fructose to trioses	32.8	30.6	29.0	19.9	21.6
Trioses to lactic acid	32.1	-	20.0	-	24.1

[a] Units are in kcal mol^{-1}. [b] Reaction steps are isomerisation of glucose to fructose, retro-aldol fragmentation of fructose into trioses, and the isomerisation of trioses to lactic acid.

A detailed reaction path analysis suggests that Al(III)-OH initially triggers the deprotonation of the hydroxyl group at C2-OH of glucose or triose, forming a water molecule on the Al centre (Fig. 9a). This is an exothermic reaction and further leads to the C1-C2 H-shift reaction. After reprotonation of the C1-O bond with coordinated water, glucose (or triose) is transformed to fructose (or lactic acid) (Fig. 9a and Figs. S11-S13, ESI†). Similar mechanisms were also proposed for the Sn-containing zeolite-catalysed aldose-ketose isomerization.[54,55] In our study, since Al(III)-OH species may stabilise its transition state in C1-C2 H-shift reaction at a lower energy stage than Sn(II)-OH (Figs. S13, S28, S33, S40, ESI†), Al(III)-OH shows better performance for the isomerisation.

The retro-aldol fragmentation of fructose is a crucial step for the cleavage of C-C bond and the formation of C_3 intermediates. This reaction step needs to overcome an energy barrier of 32.8 kcal mol^{-1} without a metal-cation catalyst, which is the highest energy demanding step in the non-catalytic transformation of glucose to lactic acid. The presence of Al(III) cation slightly lowered the energy barrier. On the other hand, the activation Gibbs energy drops from 32.8 to 19.9 kcal mol^{-1} in the presence of Sn(II) species, which is significantly lower than that in the presence of Al(III). Moreover, the activation Gibbs energy with Sn(II) was lower than that with Pb(II) (22.4 kcal mol^{-1}).[40]

Our computational analysis for the reaction path reveals that the retro-aldol fragmentation of fructose is initiated by the proton transfer from the C4-OH to C2=O (Fig. 9b and Figs. S35-S39, ESI†). The coordination of Sn(II) to oxygen atoms of fructose increases the positive charges of H atom in C4-OH.

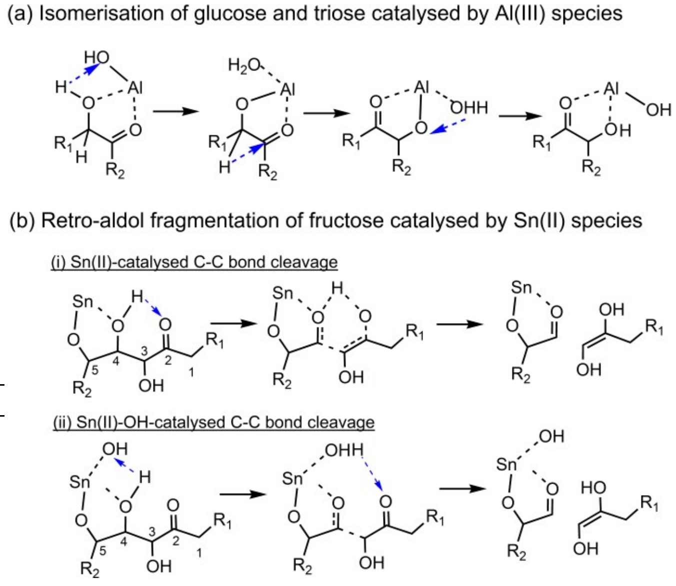
(a) Isomerisation of glucose and triose catalysed by Al(III) species
(b) Retro-aldol fragmentation of fructose catalysed by Sn(II) species
(i) Sn(II)-catalysed C-C bond cleavage
(ii) Sn(II)-OH-catalysed C-C bond cleavage

Fig. 9 Proposed reaction paths based on theoretical computations for the isomerization and retro-aldol fragmentation.

This means that Sn(II) can increase the acidity of C4-OH, therefore accelerating the proton transfer and the C-C bond cleavage. In addition, the hydroxyl group in Sn(II)-OH may also mediate the proton transfer via water forming step (Fig. 9b). However, the Sn(II) species provides a relative lower activation Gibbs energy of the transition state, thus was more favourable for the C-C bond cleavage (Figs. S37-S39, ESI†). Similar to Pb(II), Sn(II) possesses a closed shell configuration and large ionic radius (118 ppm) than many other metal cations, e.g., Al(III). This may favour its coordination with oxygen atoms in fructose and may allow it to accelerate the initial proton transfer step efficiently. Moreover, the lone electron pair ($5s^2$) of Sn(II) may also facilitate the proton transfer,[56] contributing to its outstanding performance for the cleavage of C-C bond in the retro-aldol reaction.

Under non-catalytic conditions, the dehydration of fructose can occur, giving rise to HMF. This reaction requires a activation Gibbs energy of 29.1 kcal mol^{-1},[40] which is lower than the activation barrier (32.8 kcal mol^{-1}) for the retro-aldol fragmentation in the absence of a catalyst. Thus, it is understandable that HMF is formed as a major product during the conversions of cellulose and glucose under the hydrothermal conditions without metal cations (Figs. 3 and 4). The presence of a metal-cation catalyst, in particular Sn(II), decreases the activation Gibbs energy for the retro-aldol fragmentation (Table 3), thus catalysing the precise cleavage of C3-C4 bond.

We have clarified that the pH of reaction solution is a key factor. An optimum pH value (~2.8) is required for the formation of lactic acid in the presence of Al(III) and Sn(II) cations. The appropriate pH value can avoid side reactions, e.g., acid-catalysed formation of levulinic acid and humins at lower pH values (Table 1), and may help tune the concentrations of Al(III), Sn(II) and their hydroxides such as Al(III)-OH and Sn(II)-OH. A higher pH value may result in higher fractions of hydroxides, which are beneficial to the isomerisation of glucose but unfavourable for the retro-aldol fragmentation (Table 3). This can explain why fructose was observed with relatively high selectivity at a pH value of 7.6 during glucose conversion (Table 1).

As described above, we have demonstrated that the combination of Al(III) and Sn(II) can catalyse a series of tandem reactions for the transformation of glucose into lactic acid by decreasing the activation energy of each step. It is noteworthy that the selective formation of lactic acid cannot be realised only by single Al(III) or Sn(II) catalyst. This is because of the occurrence of undesirable side reactions. For example, the Al(III) species in the form of Al(III)-OH is highly active for the isomerisation of glucose to fructose, but this species shows low efficiency for the cleavage of C-C bond of fructose. Thus, the low energy-demanding reaction, i.e., the dehydration of fructose to HMF, proceeds during the Al(III)-catalysed conversion of cellulose (Fig. 6), providing a low selectivity of lactic acid. On the other hand, the Sn(II) species cannot only enhance the isomerisation of glucose (despite not as well as Al(III) species) but also facilitate the retro-aldol fragmentation of fructose. Consequently, it is expected as an efficient catalyst for the formation of lactic acid. However, the side polymerization reactions of C_3 intermediates catalysed by Sn(II) cause the moderate selectivity of lactic acid by Sn(II) alone in water (Figs. 1 and 6). It should be noted that several papers have reported that Sn-based catalysts were efficient for the transformation of glucose, fructose and sucrose to methyl lactate in methanol media.[30-32] We speculate that alcohol may facilely react with aldehyde intermediates, forming hemiacetals, which might help to prevent the intermediates from side polymerisations. Therefore, the incorporation of Al(III) into the Sn(II)-catalysed system provides a promising way to realise the highly selective synthesis of lactic acid in water other than alcohol medium.

4. Conclusions

The present work has demonstrated that the combination of Al(III) and Sn(II) cations efficiently catalyses the selective transformation of cellulose or the related carbohydrates into lactic acid in water. Under optimized conditions, the Al(III)-Sn(II) combination could provide lactic acid yields of 65%, 81%, and 90% from cellulose, glucose and fructose, respectively. We have clarified that the transformation of cellulose into lactic acid involves a series of tandem steps including the hydrolysis to glucose, the isomerisation of glucose to fructose, the retro-aldol fragmentation of fructose into two C_3 intermediates and the selective conversion of C_3 intermediates to lactic acid. Our experimental and computational studies reveal that the Al(III) species accounts for the isomerisation of glucose to fructose via 1,2-hydride shift mechanism and the conversion of trioses to lactic acid, where the isomerisation reaction is the rate-limiting step. On the other hand, the Sn(II) species efficiently catalyses the retro-aldol fragmentation of fructose into two C_3 intermediates. The dehydration of fructose into HMF is a major side reaction in the presence of Al(III) without Sn(II), whereas the polymerisation of C_3 intermediates into humins occurs as the major side reaction in presence of Sn(II) alone. The Al(III)-Sn(II) dual cations with a molar ratio of 1/1 can cooperate with each other and work multi-functionally for the selective formation of lactic acid in water medium. The coupling of multifunctional sites, which are suitable for different elementary steps, is a useful strategy for catalyst design for high-selective chemical transformations that contain complex tandem elementary steps.

Acknowledgements

This work was supported by the National Natural Science Foundation of China (21690082, 91545203 and 21473141), the Research Fund for the Doctorial Program of Higher Education (20130121130001), the Fundamental Research Funds for the Central Universities (20720160029) and the Program for Innovative Research Team in University (IRT_14R31).

Conflicts of interest

View Article Online
DOI: 10.1039/C7GC02975F

There are no conflicts to declare.

Notes and references

1 A. Corma, S. Iborra and A. Velty, *Chem. Rev.*, 2007, **107**, 2411-2502.
2 D. M. Alonso, S. G. Wettstein and J. A. Dumesic, *Chem. Soc. Rev.*, 2012, **41**, 8075-8098.
3 M. Besson, P. Gallezot and C. Pinel, *Chem. Rev.*, 2014, **114**, 1827-1870.
4 C. Li, X. Zhao, A. Wang, G. W. Huber and T. Zhang, *Chem. Rev.*, 2015, **115**, 11559-11624.
5 R. Rinaldi and F. Schuth, *ChemSusChem*, 2009, **2**, 1096-1107.
6 H. Zhao, J. E. Holladay, H. Brown and Z.C. Zhang, *Science*, 2007, 1597-1600.
7 J. B. Binder and R. T. Raines, *J. Am. Chem. Soc.*, 2009, **131**, 1979-1985.
8 A. Fukuoka and P. L. Dhepe, *Angew. Chem. Int. Ed.*, 2006, **45**, 5161-5163.
9 C. Luo, S. Wang and H. Liu, *Angew. Chem. Int. Ed.*, 2007, **46**, 7636-7639.
10 N. Ji, T. Zhang, M. Zheng, A. Wang, H. Wang, X. Wang and J. Chen, *Angew. Chem. Int. Ed.*, 2008, **47**, 8510-8513.
11 Y. Liu, C. Luo and H. Liu, *Angew. Chem. Int. Ed.*, 2012, **51**, 3249-3253.
12 A. Wang and T. Zhang, *Acc. Chem. Res.*, 2013, **46**, 1377-1386.
13 D. An, A. Ye, W. Deng, Q. Zhang and Y. Wang, *Chem. Eur. J.*, 2012, **18**, 2938-2947.
14 R. Weingarten, W. C. Conner and G. W. Huber, *Energy Environ. Sci.*, 2012, **5**, 7559-7574.
15 M. Dusselier, P. Van Wouwe, A. Dewaele, E. Makshina and B. F. Sels, *Energy Environ. Sci.*, 2013, **6**, 1415-1442.
16 W. Deng, Q. Zhang and Y. Wang, *Catal. Today*, 2014, **234**, 31-41.
17 S. P. Teong, G. Yi and Y. Zhang, *Green Chem.*, 2014, **16**, 2015-2026.
18 W. Deng, Q. Zhang and Y. Wang, *Sci. China Chem.*, 2015, **58**, 29-46.
19 P. Maki-Arvela, I. L. Simakova, T. Salmi and D. Y. Murzin, *Chem. Rev.*, 2014, **114**, 1909-1971.
20 M. Bicker, S. Endres, L. Ott and H. Vogel, *J. Mol. Catal. A* 2005, **239**, 151-157.
21 H. Kishida, F. Jin, X. Yan, T. Moriya and H. Enomoto, *Carbohydr. Res.*, 2006, **341**, 2619-2623.
22 X. Yan, F. Jin, K. Tohji, A. Kishita and H. Enomoto, *AIChE J.*, 2010, **56**, 2727-2733.
23 G. Epane, J. C. Laguerre, A. Wadouachi and D. Marek, *Green Chem.*, 2010, **12**, 502-506.
24 X. Wang, Y. Song, C. Huang, F. Liang and B. Chen, *Green Chem.*, 2014, **16**, 4234-4240.
25 H. Choudhary, S. Nishimura and K. Ebitani, *Appl. Catal. B: Environ.*, 2015, **162**, 1-10.
26 L. Li, F. Shen, R. L. Smith and X. Qi, *Green Chem.*, 2017, **19**, 76-81.
27 C. B. Rasrendra, I. G. B. N. Makertihartha, S. Adisasmito and H. J. Heeres, *Top. Catal.*, 2010, **53**, 1241-1247.
28 J. B. dos Santos, F. L. da Silva, F. M. R. S. Altino, T. da Silva Moreira, M. R. Meneghetti and S. M. P. Meneghetti, *Catal. Sci. Technol.*, 2013, **3**, 673-678.
29 L. Zhou, L. Wu, H. Li, X. Yang, Y. Su, T. Lu and J. Xu, *J. Mol. Catal. A: Chem.*, 2014, **388-389**, 74-80.
30 M. S. Holm, S. Saravanamurugan and E. Taarning, *Science*, 2010, **328**, 602-605.
31 S. Tolborg, I. Sadaba, C. M. Osmundsen, P. Fristrup, M. S. Holm and E. Taarning, *ChemSusChem*, 2015, **8**, 613-617.
32 F. de Clippel, M. Dusselier, R. Van Rompaey, P. Vanelderen, J. Dijkmans, E. Makshina, L. Giebeler, S. Oswald, G. V. Baron, J. F. M. Denayer, P.P. Pescarmona, P. A. Jacobs and B. F. Sels, *J. Am. Chem. Soc.*, 2012, **134**, 10089-10101.
33 D. Verma, R. Insyani, Y. W. Suh, S. M. Kim, S. K. Kim and J. Kim, *Green Chem.*, 2017, **19**, 1969-1982.
34 P. Wattanapaphawong, P. Reubroycharoen and A. Yamaguchi, *RSC Adv.*, 2017, **7**, 18561-18568.
35 F. Chambon, F. Rataboul, C. Pinel, A. Cabiac, E. Guillon and N. Essayem, *Appl. Catal. B*, 2011, **105**, 171-181.
36 S. M. Coman, M. Verziu, A. Tirsoaga, B. Jurca, C. Teodorescu, V. Kuncser, V. I. Parvulescu, G. Scholz, E. Kemnitz, *ACS Catal.*, 2015, **5**, 3013-3026.
37 F. Wang, C. Liu and W. Dong, *Green Chem.*, 2013, **15**, 2091-2095.
38 F. Wang, J. Liu, H. Li, C. Liu, R. Yang and W. Dong, *Green Chem.*, 2015, **17**, 2455-2463.
39 P. J. Deuss, K. Barta and J. G. de Vries, *Catal. Sci. Technol.*, 2014, **4**, 1174-1196.
40 Y. Wang, W. Deng, B. Wang, Q. Zhang, X. Wan, Z. Tang, Y. Wang, C. Zhu, Z. Cao, G. Wang and H. Wan, *Nat. Commun.*, 2013, **4**, 2141.
41 R. F. Ribeiro, A. V. Marenich, J. C. Cramer and D. G. Truhlar, *J. Phys. Chem. B*, 2011, **115**, 14556-14562.
42 S. A. Nolen, C. L. Liotta, C. A. Eckert and R. Glaser, *Green Chem.*, 2003, **5**, 663-669.
43 J. Dijkmans, M. Dusselier, D. Gabriels, K. Houthoofd, P. C. M. M. Magusin, S. Huang, Y. Pontikes, M. Trekels, A. Vantomme, L. Giebeler, S. Oswald and B. F. Sels, *ACS Catal.*, 2015, **5**, 928-940.
44 K. Nemoto, Y. Hirano, K. Hirata, T. Takahashi, H. Tsuneki, K. Tominaga and K. Sato, *Appl. Catal. B: Environ.*, 2016, **183**, 8-17.
45 T. Mukaiyama, R. Tsuzuki and J. Kato, *Chem. Lett.*, 1983, 1825-1828.
46 B. Wang and Z. Cao, *Angew. Chem.Int. Ed.,* 2011, **50**, 3266-3270.
47 R. B. Sunoj and M. Anand, *Phys. Chem. Chem. Phys.,* 2012, **14**, 12715-12736.
48 S. J. Angyal, In Glycosicence; A. Stutz, Ed.; Springer: Berlin, 2001, **215**, 1-4.
49 C. Liu, J. M. Carraher, J. L. Swedberg, C. R. Herndon, C. N. Fleitman and J. P. Tessonnier, *ACS Catal.*, 2014, **4**, 4295-4298.
50 J. Tang, X. Guo, L. Zhu and C. Hu, *ACS Catal.,* 2015, **5**, 5097-5103.
51 V. Choudhary, A. B. Pinar, R. F. Lobo, D. G. Vlachos and S. I. Sandler, *ChemSusChem,* 2013, **6**, 2369-2376.
52 Y. Román-Leshkov, M. Moliner, J. A. Labinger and M. E. Davis, *Angew. Chem. Int. Ed*., 2010, **49**, 8954-8957.
53 W. N. P. van der Graaff, G. Li, B. Mezari, E. A. Pidko and E. J. M. Hensen, *ChemCatChem,* 2015, **7**, 1152-1160.
54 C. B. Rasrendra, B. A. Fachri, I. G. B. N. Makertihartha, S. Adisasmito, H. J. Heeres, *ChemSusChem*, 2011, **4**, 768-777.
55 G. Li, E. A. Pidko and E. J. M. Hensen, *Catal. Sci. Technol.*, 2014, **4**, 2241-2250.
56 H. Cox and A. J. Stace, *J. Am. Chem. Soc.*, 2004, **126**, 3939-3947.

View Article Online
DOI: 10.1039/C7GC02975F

Graphic abstract

View Article Online
DOI: 10.1039/C7GC02975F

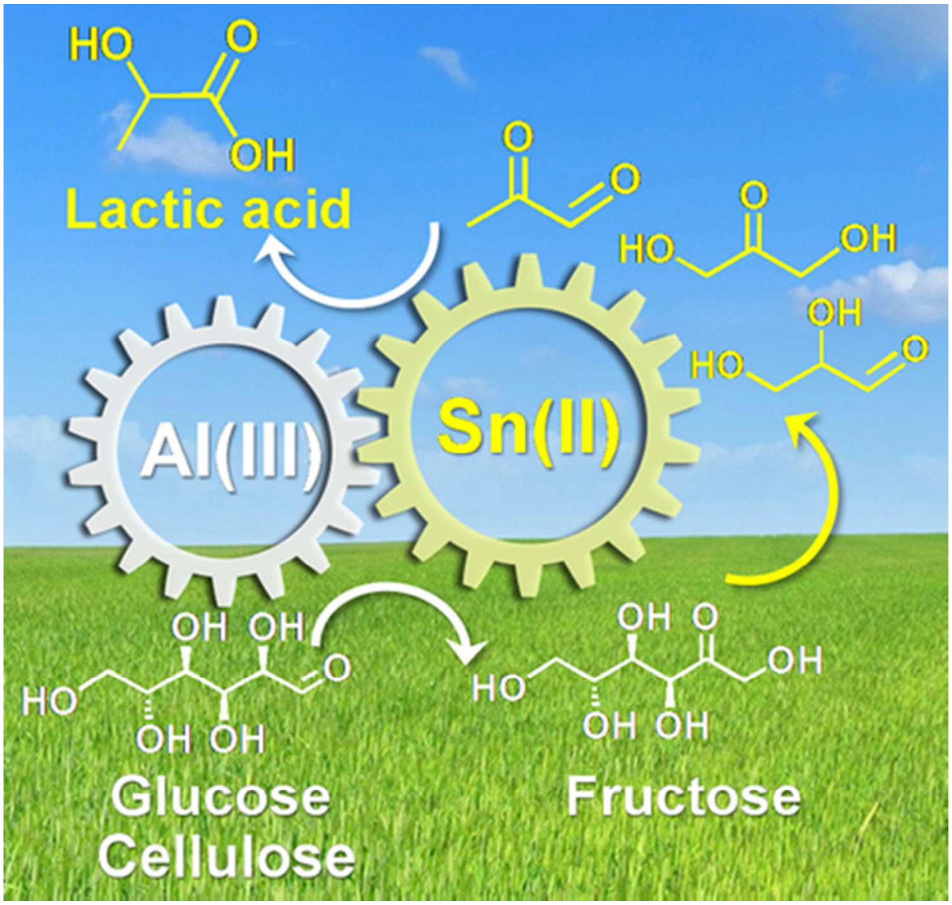

39x37mm (300 x 300 DPI)